Building and Environment 178 (2020) 106879

Contents lists available at ScienceDirect

Building and Environment

journal homepage: http://www.elsevier.com/locate/buildenv

HEAT - Human Embodied Autonomous Thermostat

Da Li [a], Carol C. Menassa [b,*], Vineet R. Kamat [b], Eunshin Byon [c]

[a] Glenn Department of Civil Engineering, Clemson University, SC, 29634, United States
[b] Department of Civil and Environmental Engineering, University of Michigan, MI, 48109, United States
[c] Department of Industrial and Operations Engineering, University of Michigan, MI, 48109, United States

ARTICLE INFO

Keywords:
Human occupants as thermostats
Thermal comfort
Personal comfort model
Physiological sensing
Physiological predictive model
Temperature setpoint optimization

ABSTRACT

The lack of thermal comfort among occupants is a common problem in built environments. Recent studies have investigated various physiological sensing and modeling approaches and demonstrated more robust thermal comfort prediction than the Predicted Mean Vote and participatory sensing methods. However, such physiological sensing approaches only work with iterative and passive Heating, Ventilation, and Air Conditioning (HVAC) control schemas which can lead to problems including uncertainties in setpoint control outcomes and interruptions to building occupants. To address this critical limitation, this paper proposes a new paradigm named Human Embodied Autonomous Thermostat (HEAT) that considers human occupants as an embodiment of smart and connected thermostats where physiological measurements in form of facial skin temperature can be used to directly communicate with and control HVAC operations for improved thermal satisfaction and reduced energy use while maintaining comfort in multi-occupancy spaces. This paradigm leverages occupants' skin temperature responses under different thermal environments and integrates two types of personal models - thermal comfort model and physiological predictive model to determine occupants' comfort, which can be represented as the thermal comfort zone and comfort probability. Based on these two metrics, three HVAC strategies are compared to demonstrate thermal comfort optimization for a group of occupants. The result suggests different setpoint options as a trade-off between overall comfort and energy use. The proposed HEAT framework can conceptually make wall-mounted physical thermostats redundant by serving as a basis for automated environment control based directly on human measurements to improve personalized human experience, well-being, and building energy efficiency.

1. Introduction

Thermal comfort among building occupants is an influential factor in human satisfaction, health, and well-being. Lack of thermally comfortable environments can lead to several problems including sick building syndrome, complaints, absenteeism, and reduced work productivity [1–4]. However, understanding thermal comfort is a challenging task as both human and environmental factors affect people's thermal sensations and preferences [5]. This problem is exacerbated in multi-occupancy environments where thermal comfort not only evolves within each occupant but also varies from one person to another. Therefore, static Heating, Ventilation, and Air Conditioning (HVAC) operation strategies recommended by industry guidelines (e.g., ASHRAE) can fail to provide an optimum thermal environment, i.e., an environment that keeps as many occupants comfortable as possible, if not all.

To address this research problem, this paper proposes the Human Embodied Autonomous Thermostat (HEAT) framework where occupants act as thermostats carrying their personal thermal profiles into a shared space (e.g., offices). This framework allows the thermal environment to be automatically optimized based on the profiles detected in the space to improve overall satisfaction and wellness without humans interacting with a physical thermostat. The proposed framework consists of two components: (1) thermal comfort sensing, which develops personal comfort models to interpret the comfort state of each occupant; and (2) thermal comfort optimization, which determines the optimum setpoint for a given group of occupants.

The remaining sections of this paper are organized as follows. Section 2 reviewed the existing literature on thermal comfort sensing and optimization and highlighted their limitations. Section 3 summarized the objectives of this paper. Section 4 presented the methodology of the HEAT framework. Section 5 compared three setpoint optimization

* Corresponding author.
E-mail addresses: dli3@clemson.edu (D. Li), menassa@umich.edu (C.C. Menassa), vkamat@umich.edu (V.R. Kamat), ebyon@umich.edu (E. Byon).

https://doi.org/10.1016/j.buildenv.2020.106879
Received 2 December 2019; Received in revised form 26 March 2020; Accepted 6 April 2020
Available online 8 May 2020

strategies using the experimental data. Section 6 discussed the results and research implications. Finally, Section 7 concluded the paper.

2. Background

Existing literature investigated thermal comfort sensing approaches to understand occupants' thermal comfort, such as the Predicted Mean Vote (PMV) model, adaptive model, human participatory sensing, and personal comfort model. These sensing approaches can be applied in multi-occupancy spaces to achieve a real-time evaluation of the overall thermal environment. Following the sensing step, various HVAC control strategies can be implemented to determine the optimum setpoint for improved thermal comfort and satisfaction.

2.1. Thermal comfort sensing

Industry standards in thermal comfort originated from the static PMV model which was based on the thermal transfer between the human body and environments [6]. Later, De Dear and Brager [7] proposed the adaptive model and suggested that occupants' behavioral and psychological adaption in naturally ventilated buildings can lead to a wider range of acceptable temperature than the PMV prediction. However, these two classic approaches are unable to reflect the "personalized" nature of thermal sensation and preference as they are both developed from the responses of a large group of human subjects.

With the rapid development of wireless sensor network, mobile devices, and ubiquitous computing, researchers also explored participatory sensing approaches, which assess thermal conditions using environmental data and the corresponding human feedback (e.g., Refs. [8–12]. This is also known as the "human-in-the-loop" approach which brings occupants' actual thermal sensations into the HVAC control process. In these approaches, thermal comfort is typically modeled using only environmental parameters. For example, Feldmeier and Paradiso [10] applied linear discriminant models to classify thermal sensations based on room temperature and humidity. Daum et al. [8] developed comfort models using logistic regression, which represents the comfort probability at different room temperatures. Similarly, Jazizadeh et al. [11] developed fuzzy models to describe the comfort probability as a function of room temperature. However, these participatory sensing approaches fail to consider the role of human physiological and behavioral factors in affecting thermal comfort, which may result in a less robust comfort prediction [13,14]. For example, the same individual with different workloads can have direct opposite thermal preferences in the same environment. Also, these approaches rely on continuous feedback from occupants to rectify comfort predictions or determine future setpoints, which is interruptive in real applications. For a detailed discussion about participatory sensing and its limitations, please refer to Li et al. [15].

To address the limitations in the above comfort sensing approaches, personal comfort models which leverage human physiological data have gained much attention in recent years [14–24,41,42]. This approach maps real-time human physiological data, such as skin temperature, heat flux, respiration, and heart rate collected from the human body, into a prediction of thermal comfort. In this paradigm, each personal model captures the "individual differences". In other words, personal models only represent the corresponding "training person" and are not intended to extrapolate to other people or an "average person". Studies such as Aryal and Becerik-Gerber [16]; Jung et al. [13]; and Li et al. [14] suggested that physiological sensing-based comfort models can achieve better prediction accuracy than models which only consider environmental data and have the potential to reduce the intrusiveness caused by human participation.

Among various human physiological signals, skin temperature has been widely adopted in existing literature as it is directly associated with thermoregulatory behaviors of the human body (e.g., vasodilation and vasoconstriction) under thermal stimuli. In practice, skin temperature can be collected from contact thermocouples [17,25], contact-less infrared thermometers [16,19], and thermal cameras [15,16,26]. Typical body parts for skin temperature measurement include wrists [14,16,24], hands [17,25], and faces [15,19,26]. Particularly, non-intrusive approaches have been proposed for comfort sensing using facial thermography collected from low-cost thermal cameras [15,23,27]. For details about the instruments and measurement accuracy, please refer to Ref. [15].

2.2. Thermal comfort optimization

Once the overall thermal comfort in a built environment is evaluated, a closely related question may arise, which is, how to adjust HVAC settings to optimize the overall thermal comfort and satisfaction? This question has been investigated in existing literature such as Daum et al. [8]; Deng and Chen [18]; Erickson and Cerpa [9]; Feldmeier and Paradiso [10]; Jazizadeh et al. [11]; Jung and Jazizadeh [28]; Li et al. [14]; and Purdon et al. [12]. The main strategy adopted in these studies is adjusting thermostat setpoints to increase or decrease room temperature. This is because room temperature directly and significantly affects the perceived thermal comfort compared to other environmental factors, such as relative humidity, and can be easily controlled by the thermostat [29]. Also, studies observed that variations in relative humidity are a byproduct of setpoint adjustment in real operational environments where relative humidity shows a negative correlation with room temperature [13,23]. Moreover, room temperature can be measured by regular temperature sensors, which are low-cost compared to black-globe thermometers for mean radiant temperature. As a result, only room temperature setpoint is considered as a control variable in many HVAC strategies.

In general, existing studies that aim to optimize the setpoint for improved thermal comfort can be summarized into two categories: (1) a passive and iterative control process which implements a corrective temperature in each step; and (2) a closed-form optimization that attempts to achieve the optimum setpoint in one step.

Studies in the former category typically leverage the feedback or thermal vote from occupants over time. For example, Erickson and Cerpa [9] calculated the corrective temperature using the PMV model to offset discomfort votes received in each decision cycle, which is set at 10 min. This corrective temperature then updated the current setpoint to provide additional heating or cooling to restore a thermally neutral state. Purdon et al. [12] also leveraged this voting mechanism (e.g., −1 for cooler, 1 for warmer) where the net vote, i.e., the sum of votes from all occupants, was calculated in each cycle. The room temperature will decrease by a fixed step of 1 °C for a negative net vote, which indicates a lower temperature is preferred, and vice versa. In Li et al. [14]; occupants' personal comfort models were applied in the HVAC control loop to update the setpoint. If a negative or positive net thermal vote was collected in a decision cycle (i.e., every 30 min), the control algorithm will evaluate the new setpoint (i.e., previous setpoint ±1 °C) using each occupant's comfort model. A corrective temperature will be implemented if more occupants were predicted comfortable under the new setpoint. As discussed in these three example studies, this HVAC control schema is an iterative process as continuous corrective steps are needed when occupants provide new thermal votes. This is also a passive process as it is unable to proactively determine the optimum setpoint for the future. As a result, this schema can lead to longer discomfort time due to its trial-and-error nature and also make the setpoints oscillate over time, which may lead to energy waste.

Another category of HVAC control strategy uses environmental factor-based comfort models to find a closed-form solution for the optimum setpoint [28,30]. In this schema, as comfort models directly associate room temperature with thermal comfort, a closed-form solution, which outputs the optimum setpoint that maximizes an objective function (e.g., the number of comfortable occupants), can be directly obtained [8,11,28]. For example, Jung and Jazizadeh [28] compared

three HVAC control strategies in determining the optimum setpoint. In this study, personal comfort models, which measure the probability of being comfortable (i.e., comfort probability) as a function of room temperature, are developed using the Gaussian distribution. Specifically, this study introduced the concept of thermal sensitivity, i.e., the increased or decreased comfort probability caused by variations in room temperature. Using this metric, the optimum setpoint is chosen to maximize the sum of comfort probability of all occupants. This study provides useful insights into the HVAC control by addressing the optimization problem in a probabilistic view and considering the different thermal sensitivities to hot and cold stimuli.

However, the one-step HVAC optimization strategies such as Jung and Jazizadeh [28] cannot directly integrate with human physiological sensing-based comfort models. In this case, a major challenge should be addressed - the uncertainties in occupants' thermal comfort under a new setpoint, which result from the unknown effect of updated thermal environments on human physiological parameters. For example, in a scenario where skin temperature is used for comfort prediction, personal comfort models can continuously predict the thermal preference or its probability as long as a new skin temperature measurement is collected. If these models predict "occupants prefer warmer" and the setpoint is increased by a fixed step (e.g., 1 °C) accordingly, it is unknown how much people's skin temperature will be affected by this adjustment, resulting in uncertainties in setpoint control outcomes. In other words, physiological sensing-based comfort models enable evaluations of current comfort state but cannot make predictions about the future. Therefore, it only works with the iterative and passive HVAC control strategy introduced above.

Fig. 1 illustrates this problem using an example environment occupied by three occupants (denoted as *id*1, *id*2, and *id*3). In this example, the setpoint is initially set at 24 °C at time *t*. Occupants' physiological data at time *t* are collected (denoted as T^t_{id1}, T^t_{id2}, T^t_{id3}), and predictions show that two of them prefer a warmer environment and one prefers a cooler environment. As a result, the system decides to increase the setpoint by 1 °C, which will be implemented at time $t+1$. However, as the impact of this adjustment on the physiological parameter is unknown at time *t*, the system has no knowledge about occupants' future physiological conditions at time $t+1$ (denoted as T^{t+1}_{id1}, T^{t+1}_{id2}, T^{t+1}_{id3}), and thus fails to predict future thermal comfort states that will result from this adjustment. Therefore, three possible outcomes of this adjustment (i.e., increase the setpoint by 1 °C) can be encountered at time $t+1$ including an insignificant control (the majority still prefer warmer), a promising control (the majority now feel comfortable), and an overshoot control (the majority start to prefer cooler). If either the insignificant or overshoot outcome occurs, then an additional adjustment has to be implemented by using the current physiological data at time $t+1$, and its corresponding impact is unknown until time $t+2$.

Also, existing optimization strategies typically associate each occupant with a single and fixed comfort zone (e.g., occupant #1 is always comfortable when room temperature is between 23 and 26 °C) [8,11,28], which fails to acknowledge the same occupant can have different comfort zones as his/her physiological states change over time (see Fig. 2). A promising approach to address this limitation is to include human factors to indicate an occupant's current physiological state [14], and then determine the optimum setpoint based on the comfort zone associated with the identified state.

Therefore, to address the limitations in existing studies and achieve a proactive HVAC control, it is important to consider human physiological data and also understand the impact of room temperature variations (or other environmental variables if applicable) on physiological parameters in the personal comfort model. To this end, this paper presents an approach to predict occupants' future physiological responses and demonstrates its integration with personal comfort models to determine optimum setpoints. The objectives of this paper and the methodology are presented as follows.

3. Objectives

This study leverages the merits of physiological comfort sensing and fills an important research gap that prevents its integration in HVAC control strategies. The resulting HEAT framework can achieve a robust thermal comfort prediction through physiological sensing and proactively determine the optimum setpoint of multi-occupancy environments. The specific objectives of this paper include:

- Demonstrate how to integrate physiological predictive models and personal comfort models to evaluate an occupant's comfort (i.e., thermal comfort zone or comfort probability) under a new setpoint, particularly when the physiological sensing is adopted.
- Develop a modeling approach to interpret human physiological states (e.g., skin temperature) under different environmental conditions (e.g., room temperature).

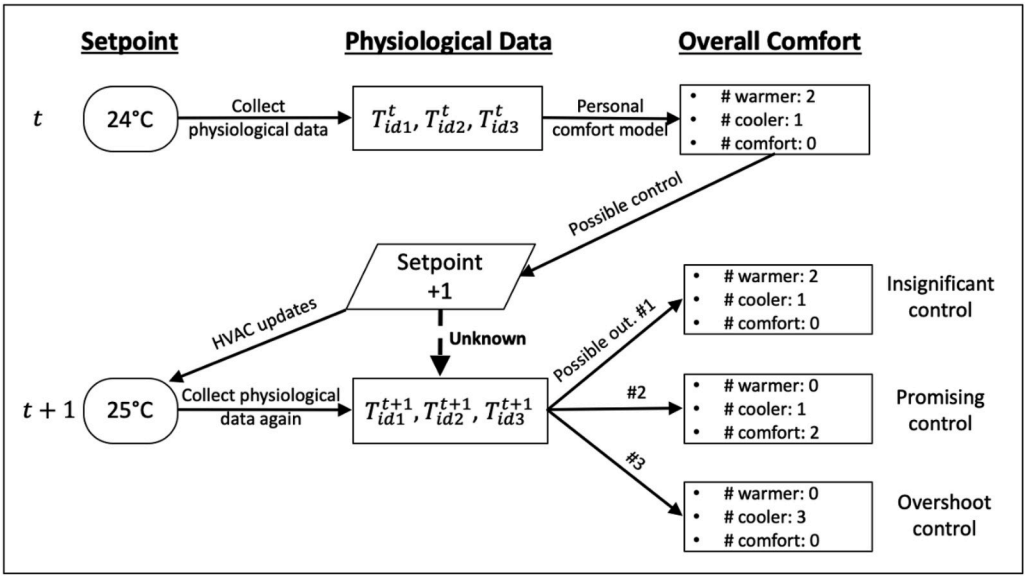

Fig. 1. The HVAC control steps when using physiological sensing-based models.

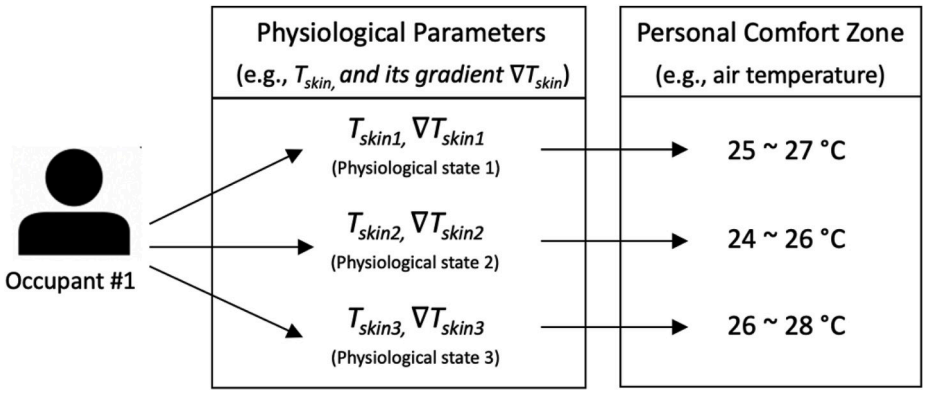

Fig. 2. Determining an occupant's thermal comfort zone based on physiological states.

- Demonstrate how HVAC control strategies can optimize thermal comfort and energy consumption in a multi-occupancy environment using each occupant's thermal comfort zone and comfort probability.

4. Methodology

This paper uses facial skin temperature and room temperature as the human physiological parameter and environmental parameter, respectively, to demonstrate the HEAT framework. Fig. 3 shows an overview of the framework, which can be decomposed into two steps including (1) occupants' thermal comfort prediction using facial skin temperature, i.e., the "sensing" step; and (2) determination of optimum setpoints based on the overall comfort prediction, i.e., the "optimization" step. The former sensing step can be represented by a model f which maps an occupant's skin temperature T_{skin} into his/her thermal comfort state TC (Eq. (1)), which can be a regression (e.g., thermal sensation with numerical scales), classification (e.g., thermal preference with categorical scales), or a probability distribution (e.g., probability of being comfortable). The model g, on the other hand, is the missing physiological predictive component that bridges the new setpoint T_{room} which is a possible control strategy and the projected skin temperature T_{skin} under this new setpoint (Eq. (2)). By chaining these two models f and g, an occupant's thermal comfort under a new setpoint can be predicted with physiological sensing as an intermediate step (Eq. (3)). The approaches to develop each model are presented in the following subsections.

$$f : T_{skin} \rightarrow TC, \tag{1}$$

$$g : T_{room} \rightarrow T_{skin}, \tag{2}$$

$$f(g) : T_{room} \rightarrow TC, \tag{3}$$

4.1. Personal thermal comfort models

Thermal comfort prediction is typically considered as a classification problem, which predicts an occupant's thermal sensation or preference at different conditions. As a result, personal comfort models (i.e., model f) can be trained using various classification algorithms including the Random Forest (RF), Support Vector Machine (SVM), Logistic Regression (LR), and Classification Tree (Ctree) [8,13,14,17,31–34]. Among

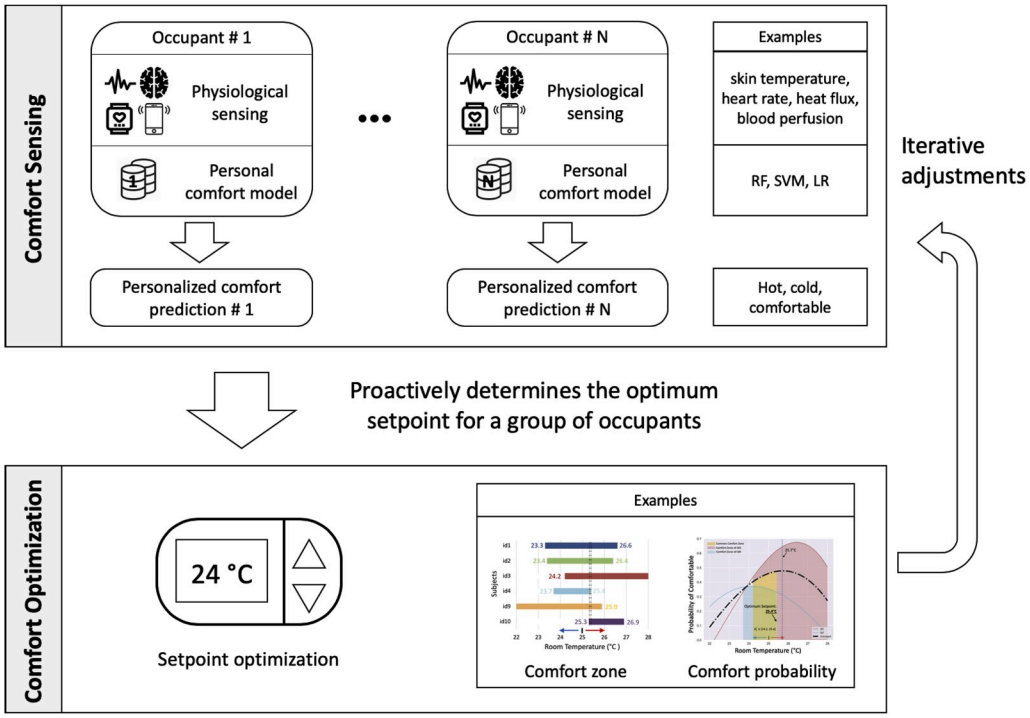

Fig. 3. An overview of the HEAT framework for thermal comfort sensing and optimization.

these approaches, studies such as Li et al. [32] and Kim et al. [31] suggested that the RF algorithm generally produces better comfort prediction accuracy than others. RF trains a collection of bagged decision trees using a random subset of features on each split and is robust to outliers and high dimensional datasets. However, one major drawback of RF is the low interpretability [35]. On the other hand, thermal comfort can also be represented in a probabilistic distribution using LR, Fuzzy Logic models, or Bayesian Networks when the number of features is small [8,11,28–30] and [36]. This approach offers significant model interpretability as changes in thermal comfort probability, which is a useful metric to determine the optimum setpoint, can be easily associated with variations in features (e.g., room temperature). As a result, this paper adopts LR to develop personal comfort models. However, other modeling approaches are also feasible and do not limit the implications of the results presented in this paper.

LR uses a logistic function to predict the probability (p) that an event happens. The basic form of LR is shown in Eq. (4) where the log-odds of an event, $\log\left(\frac{p}{1-p}\right)$, is modeled as a linear combination of input variables x's, and coefficients β's are estimated from the input data. LR is typically used to predict a binary class (e.g., an event happens or not) and an event is typically classified as 1 (an event happens) if the probability p is greater than a pre-specified threshold, e.g., 0.5 [37].

$$\log\left(\frac{p}{1-p}\right) = \beta_0 + \beta_1 \cdot x_1 + \ldots + \beta_n \cdot x_n, \tag{4}$$

LR can also be generalized to predict events with multiple classes, which is also known as the multinomial logistic regression. In this paper, the input variable is occupants' facial skin temperature, and the output variable is the corresponding thermal comfort which has three categorical values including uncomfortably hot, comfortable, and uncomfortably cold.

To develop personal comfort models, we used the FLIR Lepton thermal camera to continuously measure occupants' facial skin temperature from six regions (i.e., forehead, cheeks, nose, mouth, ears, and neck) [15]. FLIR Lepton is a low-cost factory calibrated thermal camera [38]. Details about this camera and its radiometric accuracy can be found in Li et al. [15] and Aryal and Becerik-Gerber [16]. The experimental protocol consists of three scenarios, i.e., heating, cooling, and steady-state conditions (see Fig. 4). Occupants' thermal votes were recorded using a three-point thermal preference scale (i.e., prefer warmer, cooler, or neutral) every three minutes in each scenario. This three-point scale has been widely used in literature to represent the ground-truth responses for training personal models [15,16,28]. In this paper, data from ten participants are used to demonstrate the proposed HEAT framework. All participants are university students aged between 22 and 27 and were healthy at the time of the experiment. The testbed is a student research office which does not have a window. The thermostat in the testbed can adjust the room temperature between 22 and 28 °C. For more details about the experiment setup, subject recruitment, and protocols, please refer to Li et al. [15].

In this paper, cheek skin temperature is adopted as an example input variable of personal comfort models as it is found to be indicative of thermal comfort in previous experiments [15]. However, other skin temperature features can also be used to develop these models (e.g., nose, ear or average across face skin temperature).

For each subject, we collected 180 data points during the experiment. It is worth noting that for personal comfort models, the sample size which affects model robustness is the number of data points of each subject, i.e., the number of feedback or thermal votes collected from each subject, rather than the total number of subjects. Fig. 5 shows the thermal votes of subjects and their corresponding cheek temperature. In this figure, "+1" denotes uncomfortably cold (i.e., prefer warmer), "0" denotes being comfortable, and "-1" denotes uncomfortably hot (i.e., prefer cooler). It can be observed that subjects generally feel cold when their cheek temperature is low, and vice versa. However, a few exceptions exist in subjects 6, 7 and 8 where the cheek temperature has some "vacuum regions". For example, for subject 6, the cheek temperature between 31 and 32 °C is not observed. This is because the dataset of each subject consists of three scenarios (i.e., heating, cooling, and steady-state). Despite similar skin temperature and thermal vote patterns exist in each individual scenario, the skin temperature might not be continuous in its full range when data from three scenarios are combined. This observation can be caused by breaks between two experimental scenarios (heating to cooling) when subjects' skin temperature changes significantly. This situation can cause problems when using LR for comfort profiling, which will be discussed later in this section.

Based on the data presented in Fig. 5, personal comfort models can be developed using LR. As shown in Fig. 6, the green, blue, and red curves represent a subject's probability of being comfortable, uncomfortably cold, and uncomfortably hot respectively at different cheek temperatures. In this probabilistic representation, a subject is predicted as comfortable if the comfort probability is greater than the probability at the other two conditions. For example, Id 1 has an approximately 0.5 probability of feeling comfortable when his/her cheek temperature is 33 °C, which is higher than the probabilities of uncomfortably cold (probability < 0.4) and hot (probability < 0.2). Therefore, Id 1 is predicted as comfortable at this cheek temperature. Accordingly, the range of cheek temperature associated with the comfortable state is obtained (highlighted in a yellow region). As shown in Fig. 6, subjects can have different comfort ranges of cheek temperature. For example, subjects 3 and 8 have a much wider range than subject 4, which indicates they may have a higher tolerance over the variations in room temperature. After developing each subject's personal comfort model, ten-fold cross-validation is performed to obtain the classification accuracy (3 possible categories). The result is shown in Table 1. If the ground truth data (collected from occupants' feedback during the data collection phase) show this person to be indeed comfortable when his/her cheek temperature is 33 °C, then this prediction is correct. The sum total of correct predictions divided by the total number of predictions made for this individual determines the prediction accuracy shown in the table.

As shown in Table 1, personal comfort models for subjects 5, 7 and 8 have low classification accuracy. We have the following observations: comfort models for subjects 6 and 7 do not indicate a comfort range and subject 8 does not have a lower bound (see Fig. 6). This scenario results from the discontinuous cheek temperature data discussed above. A solution to this problem is to use the skin temperature of other facial regions in comfort profiling. For example, Fig. 7 shows subject 8's comfort models using six different facial regions. It can be seen that both ear and neck models indicate a comfort range, which can be used to substitute

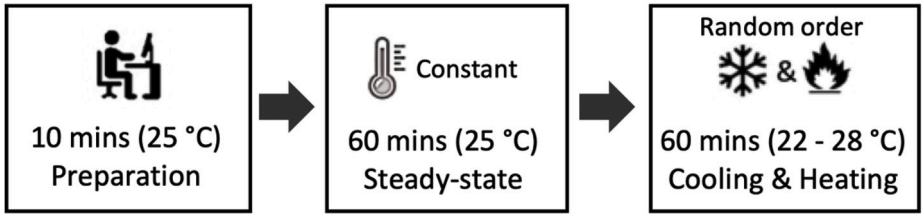

Fig. 4. Experiment Protocol in Li et al. [15].

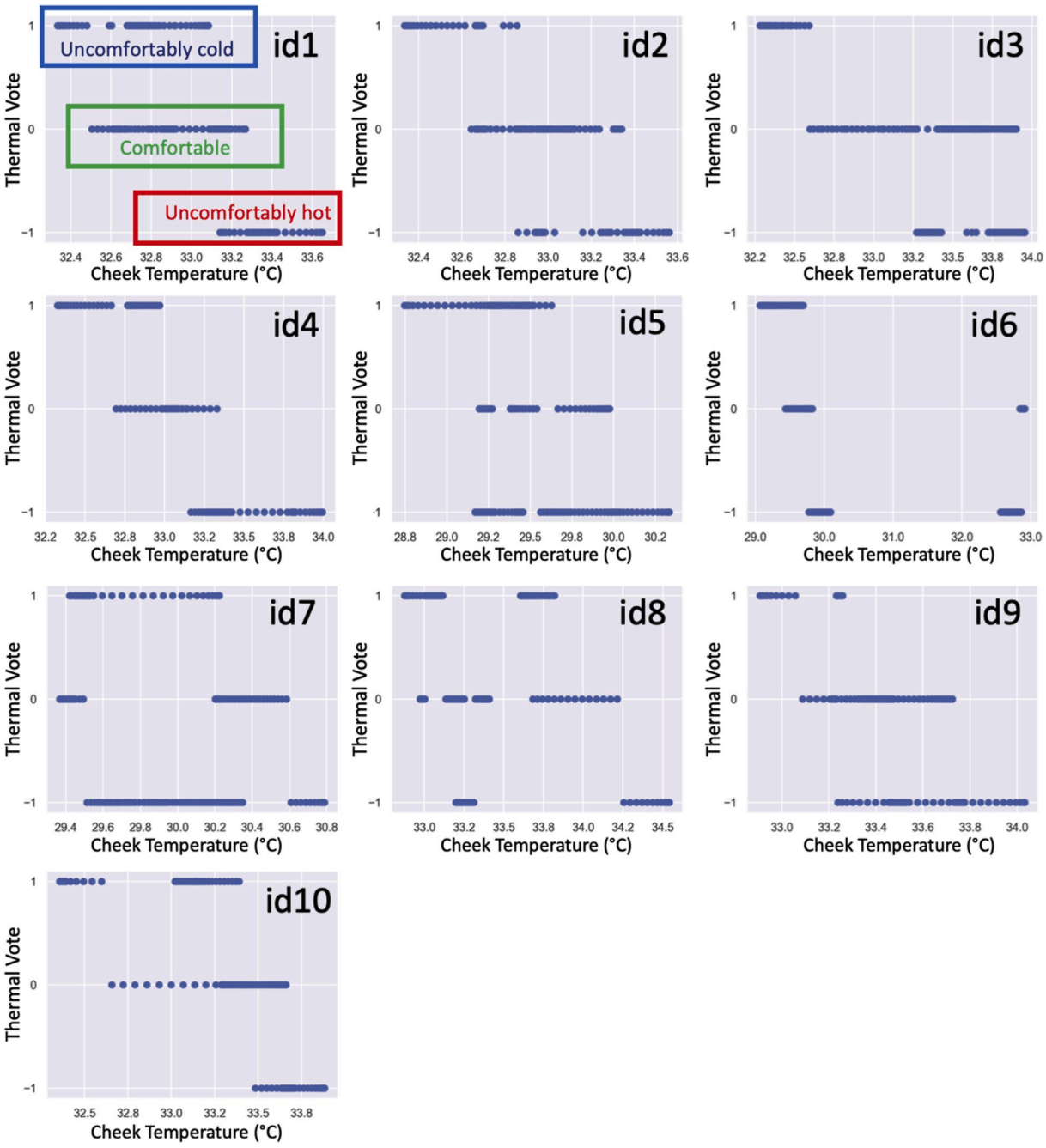

Fig. 5. Thermal votes of each subject and the corresponding cheek temperatures.

the cheek region. For subject 5, due to the imbalanced feedback which has fewer comfort votes than discomfort votes, as well as the significant overlap between cheek temperatures in different comfort conditions, the probability of being comfortable is always lower than the other two conditions. In other words, the LR model with a single input feature is not suitable for this particular subject, and more complex models such as ensemble models (e.g., Random Forest, XGBoost) may be considered.

4.2. Physiological predictive models

The physiological predictive model (i.e., model g) predicts the resulting skin temperature (or other physiological parameters) under different room temperatures, which enables personal comfort models to evaluate the impact of a new setpoint before implementation. In this model, the output variable skin temperature is affected by multiple factors, such as room temperature (i.e., the direct input variable of interest), personal variations (i.e., skin temperature variations across different subjects), and the conditioning mode (i.e., under heating or cooling states) due to subjects' different thermal sensitivities to hot and cold stress.

The linear mixed model (LMM), also known as the hierarchical model, is adopted to develop physiological predictive models. Unlike the ordinary linear regression, LMM not only considers variations that are explained by input variables of interest, i.e., the fixed effects, but also accounts for variations resulted from random samples from the population, which are called random effects. A matrix form of the LMM is shown in Eq. (5).

$$y = X\beta + Zu + \varepsilon, \tag{5}$$

with

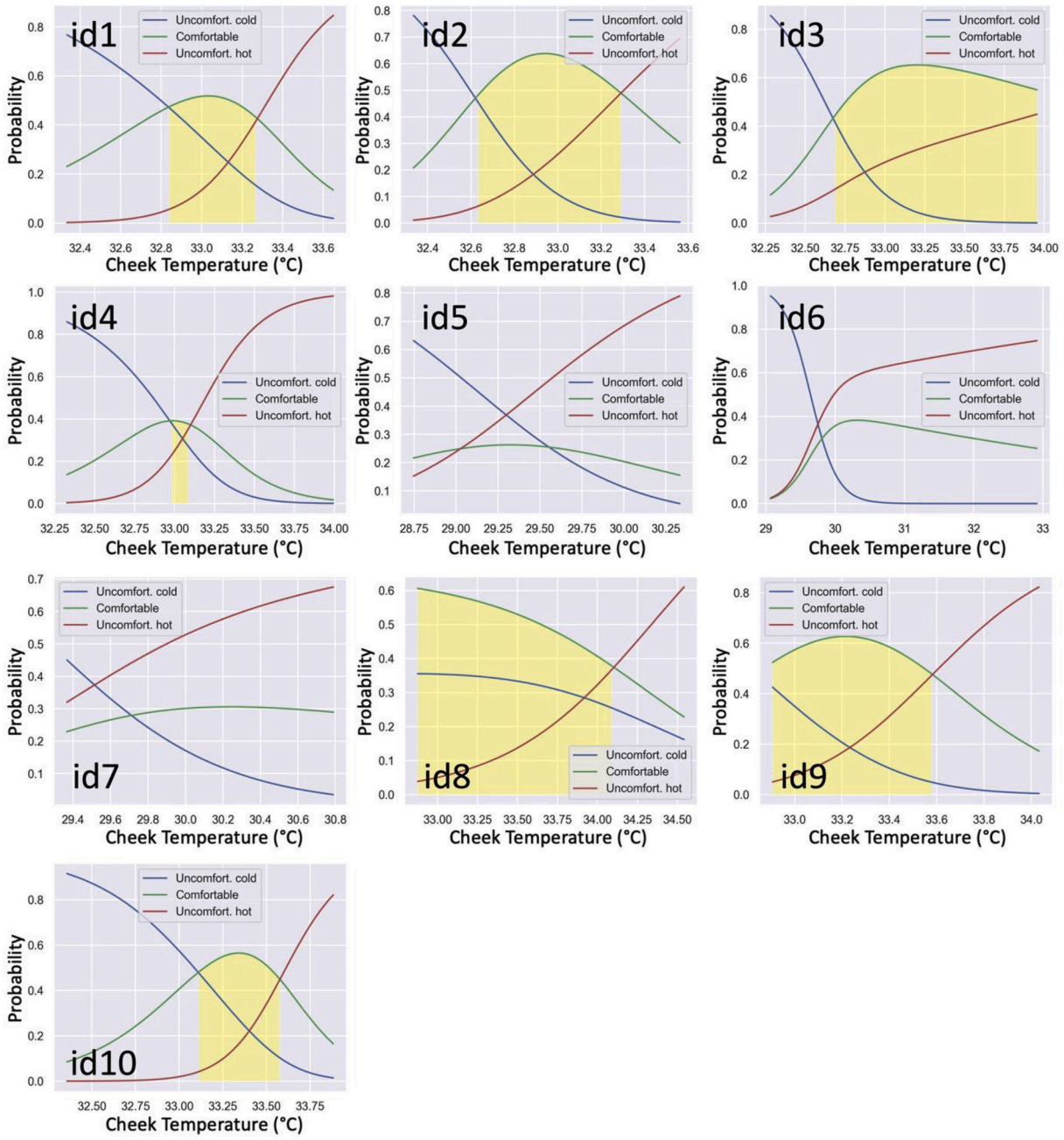

Fig. 6. Personal Comfort Model for Each Subject (yellow region denotes the range of cheek temperature when a subject feels comfortable). (For interpretation of the references to colour in this figure legend, the reader is referred to the Web version of this article.)

Table 1
Prediction accuracy of personal comfort models.

Id	1	2	3	4	5	6	7	8	9	10
Accuracy	0.70	0.78	0.70	0.81	0.41	0.78	0.51	0.58	0.66	0.81

$$u \tilde{} \mathcal{N}(0, G),$$

where y is a vector of responses, β is the unknown vector of fixed effects, u is the unknown vector of random effects which is assumed to follow a Gaussian distribution, X and Z are the design matrices, respectively, corresponding to β and u, ε is a vector of error terms, G is the variance-covariance matrix of random effects.

In statistical studies, human subjects are often used as a random effect as introducing this term accounts for individual differences between subjects [39]. In this paper, LMM lies between the ordinary linear regression, which uses aggregated sample data to train a single model (i.e., assuming each data point is independent and develop one model using all subjects' data) and the fully personalized model, which separately develops a model for each subject only using personal data. In the former case, the subject-to-subject heterogeneity is ignored and only the common patterns are captured. For the latter, on the other hand, one's personalized model does not use the information from other subjects,

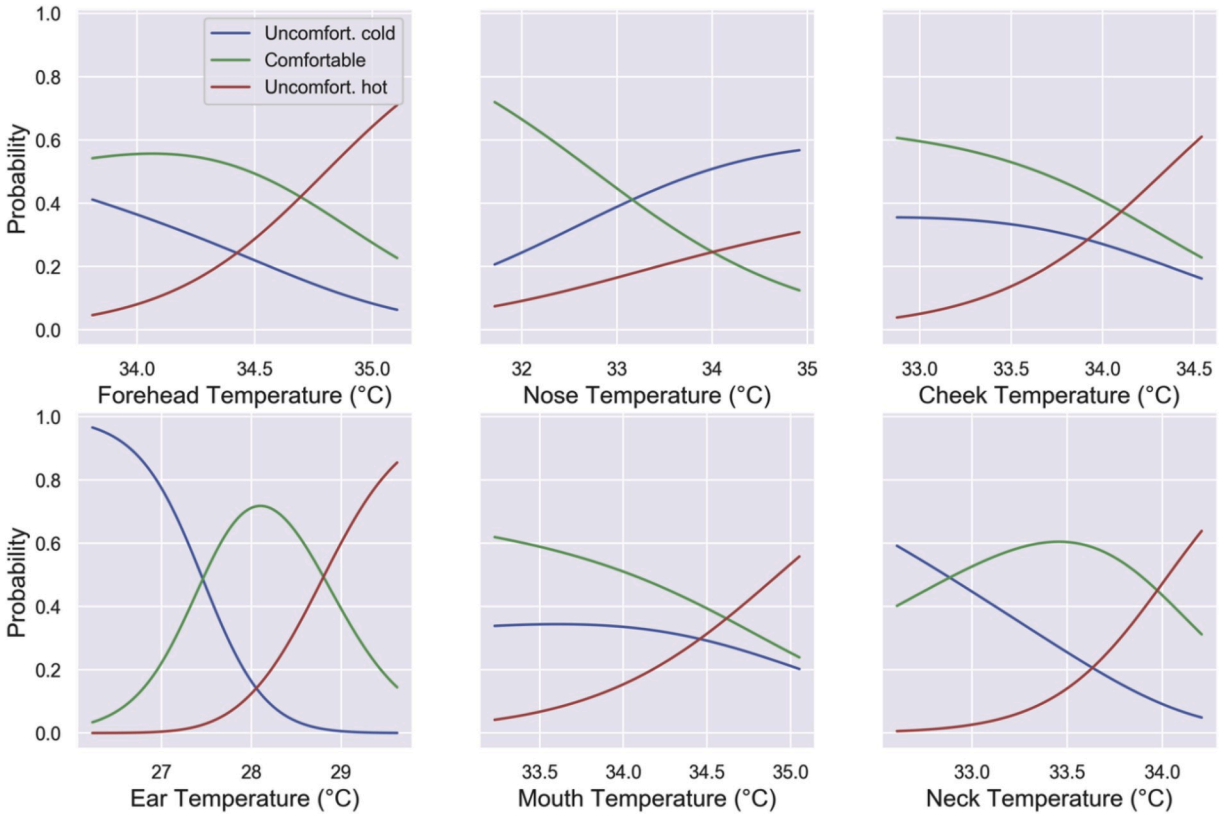

Fig. 7. Thermal comfort models for subject 8 using different facial regions.

which can lead to less robust models if each subject has a small sample size. LMM addresses these two problems by acknowledging both differences and commonalities among subjects [39]. As a result, for physiological predictive models, LMM is adopted as subjects share similarities in skin temperature variations under heating or cooling scenarios; while for the thermal comfort prediction, personal models are developed as thermal votes are subjective which may vary significantly across subjects.

The LMM models are developed using the *R* package (version 1.2). Subjects' cheek temperature from heating and cooling scenarios is used to train physiological predictive models as the skin temperature in these two scenarios changes with the room temperature. Considering the aforementioned observations, we build the LMM for skin temperature prediction where human subjects are considered as a random effect, as follows.

$$y_{ij} = \beta_0 + \beta_1 \cdot R_{ij} + \beta_2 \cdot S_{ij} + \beta_3 \cdot R_{ij} S_{ij} + b_0 + b_1 \cdot R_{ij} + b_2 \cdot R_{ij} S_{ij} + \varepsilon_{ij}, \quad (6)$$

where y_{ij} is the i^{th} subject's corresponding j^{th} skin temperature measurement at a new setpoint R_{ij}; and S_{ij} is the conditioning mode which is a binary variable (1 for cooling, 0 for heating) when the measurement is collected. The coefficients β_0 to β_3 represent the fixed effects to quantify the common pattern among multiple subjects, whereas b_0 to b_2 represent the random effects. Note that we include the interaction term $R_{ij}S_{ij}$ to account for different slopes in response to the room temperature change. We add random effects to both slopes and intercepts in order to fully characterize the heterogeneity on how each subject's skin temperature responds to the room temperature and its change.

Fig. 8 shows the physiological predictive models for cheek temperature in cooling and heating scenarios, respectively. It is worth noting that the models will look different if a different facial region is chosen. In this case, the proposed methods (Logistic Regression and Linear Mixed Model) can still be applied using data collected for the facial region of choice. In Fig. 8, The slope and intercept for each subject's model are presented in figure legends where two decimal places are kept. However, this does not mean the skin temperature is measured at 0.01 °C level by the thermal camera. As subjects 5 to 8's comfort models are less indicative (discussed in Section 4.1), physiological models of the remaining six subjects are retained in this figure. The RMSE of skin temperature prediction is 0.14 °C. The summary of fixed and random effects is presented in Table 2 and Table 3.

We make two major observations. First, subjects have different skin temperature responses to setpoint changes. For example, subject 3 is most susceptible to cold stress and will decrease cheek temperature by 0.35 °C for every 1 °C drop in room temperature; while subjects 1 and 9 have a smaller temperature gradient of 0.19 °C. This result echoes the need for personalized prediction models. Second, as indicated by the slopes, the skin temperature sensitivity is different in cooling and heating scenarios even for the same subject. From our data, skin temperature changes more rapidly when the room is cooling down as larger gradients are observed. This observation suggests that skin temperature varies in a smaller range in the heating scenario, which might be caused by the slower response time of HVAC systems in the testbed [15]. However, it should be noted that physiological models are only defined when the room temperature is between 22 and 28 °C (i.e., the range of room temperature in the experiment). These models may not be extrapolated to room temperature which is outside of this range.

5. Thermal comfort optimization strategies

As personal comfort models and physiological predictive models are developed, chaining them enables the prediction of each subject's thermal comfort including (1) thermal comfort zone, i.e., the range of temperature setpoints that keeps a subject comfortable; and (2) thermal comfort probability, i.e., the probability distribution of a subject feeling comfortable across the feasible setpoints. Based on these two metrics, three comfort optimization strategies are proposed below.

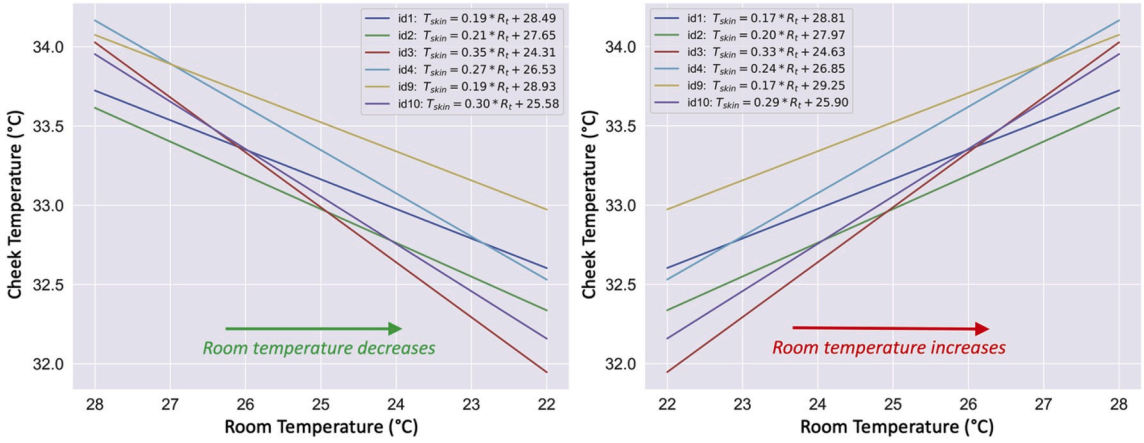

Fig. 8. Linear Mixed Models for Cheek Temperature in the Cooling and Heating Scenarios (left: cooling scenario[11]; right: heating scenario).

Table 2
Estimates of the fixed effects.

Fixed effects	Estimate	Std. Error	*t* value
Intercept	26.62	0.64	41.31
R_{ij}	0.21	0.02	11.52
S_{ij}	−0.32	0.16	−2.00
$R_{ij}S_{ij}$	0.03	0.02	1.70
Correlation	Intercept	R_t	S_t
R_{ij}	−0.690		
S_{ij}	−0.115	0.162	
$R_{ij}S_{ij}$	0.051	−0.311	−0.368

Table 3
Estimates of the random effects.

Groups	Name	Std. Dev.
Subject	Intercept	2.11
	R_{ij}	0.06
	$R_{ij}S_{ij}$	0.05
Residual		0.16

Strategy 1: The optimum setpoint should maximize the percentage of comfortable occupants in the environment, as shown in Eq. (7):

$$Setpoint^* = \underset{T \in R_t}{\operatorname{argmax}} \frac{1}{n} \sum_i Comfort_i(T) \tag{7}$$

where $Setpoint^*$ is the optimum setpoint selected by this strategy, R_t is a set of feasible setpoints in a multi-occupancy environment, n is the number of occupants, $Comfort_i(T)$ is a binary thermal comfort prediction for subject i, which is 1 if subject i is comfortable at a given setpoint T, and 0 otherwise. If multiple peaks exist, the optimum setpoint is chosen based on seasons, i.e., a higher setpoint for cooling seasons and vice versa for heating seasons.

Strategy 2: If there are multiple peaks in the results of strategy 1, the optimum setpoint should also maximize the average thermal comfort probability in the environment, as shown in Eq. (8):

$$Setpoint^* = \underset{T \in R_t^*}{\operatorname{argmax}} \frac{1}{n} \sum_i Prob_i(T) \tag{8}$$

where R_t^* is the selections of strategy 1, i.e., the range of setpoints that can keep most of the subjects comfortable in a multi-occupancy environment, $Prob_i(T)$ is the thermal comfort probability of subject i at a given setpoint T. Similar to strategy 1, the optimum setpoint depends on seasons if there is a tie in average thermal comfort probability.

Strategy 3: The optimum setpoint should maximize the average thermal comfort probability in strategy 2 with constraints in the HVAC energy consumption, as shown in Eq. (9). We use the thermostat setpoint as a proxy of the energy consumption.

$$Setpoint^* = \underset{T \in R_t^*}{\operatorname{argmax}} \{\alpha Comfort\_score - (1-\alpha) Energy\_score\} \tag{9}$$

with

$$Comfort\_score = \frac{\sum_i Prob_i(T)}{\max\limits_{T \in R_t^*} \sum_i Prob_i(T)}$$

$$Energy\_score = \left| \frac{R_{base} - T}{R_u - R_l} \right|$$

where α is the weight of thermal comfort which ranges from 0 to 1. A larger α implies more weight is given to thermal comfort than energy consumption. If $\alpha = 1$, strategy 3 only focuses on maximizing thermal comfort, which will yield the same setpoint as strategy 2. On the contrary, if $\alpha = 0$, strategy 3 focuses on making most of the occupants comfortable with the least energy use, which will choose the setpoint in R_t^* that is close to the baseline setpoint R_{base}. By tuning α, a trade-off can be found between thermal comfort and energy consumption. R_u and R_l are the upper and lower bound of the feasible setpoints, which are 28 °C and 22 °C in this paper, respectively. $|\cdot|$ is the absolute value. In this paper, we assumed 22 °C and 28 °C as the baseline setpoints for heating and cooling seasons, respectively, to represent the lowest energy consumption scenarios. Other baseline setpoints can be chosen by researchers for different climate zones. $|R_{base} - T|$ denotes the distance between the baseline setpoint and a candidate setpoint. Setpoints further away from the baseline indicate more energy use because additional cooling or heating is needed.

The following sections demonstrate these three thermal comfort optimization strategies using subjects' data discussed in Section 4.

5.1. Thermal comfort optimization using strategy 1

To determine the optimum setpoint, we assume the room temperature is originally set at 25 °C according to conventional settings (which is the median of our experimental temperature between 22 °C and 28 °C) in a multi-occupancy environment. All feasible setpoints are then searched from 25 °C to 28 °C (i.e., heating scenario) and from 25 °C to

22 °C (i.e., cooling scenario) at a step size of 0.1 °C. Although the actual HVAC systems may not allow a 0.1 °C adjustment, this assumption does not lose implications in real applications as thermal environments at two adjacent integer setpoints can be compared to choose the optimum and feasible setpoint.

When applying strategy 1, the thermal comfort zone of each subject is calculated, which is denoted as the horizontal bar in Fig. 9. In this figure, each subject's comfort zone is determined by first finding the corresponding skin temperature at a given setpoint using the physiological predictive model and then evaluating the thermal comfort states (i.e., uncomfortably hot, comfortable, and uncomfortably cold) through the personal comfort model. If the probability of being comfortable is the highest, this setpoint is added to the subject's comfort zone. Once all subjects' comfort zones are identified, the optimum setpoint will be selected to pass as many comfort zones as possible in a multi-occupancy environment. As shown in Fig. 9, for the six subjects in our experiment, 25.3 °C and 25.4 °C are selected as all subjects are comfortable at these two setpoints.

5.2. Thermal comfort optimization using strategy 2

For strategy 2, thermal comfort probabilities (i.e., the probability of being comfortable) are calculated in addition to thermal comfort zones. Thermal comfort probabilities are denoted as bell curves in Fig. 10. The average comfort probability can be obtained by averaging the probability distributions of all subjects (denoted in the black dash-dotted line). As strategy 1 suggests both 25.3 °C and 25.4 °C (i.e., R_t^*) yield the same number of comfortable subjects, the average comfort probabilities at these two setpoints are then compared. As setpoint 25.4 °C yields a higher average comfort probability than 25.3 °C, it is selected as the optimum setpoint for these six subjects.

5.3. Thermal comfort optimization using strategy 3

For strategy 3, two components, including a comfort score and an energy score, need to be calculated. The comfort score (*Comfort_score*), which ranges from 0 to 1, is the overall comfort probability at a given setpoint over the highest comfort probability achieved in range R_t^*. The energy score (*Energy_score*), which also ranges from 0 to 1, is the absolute value of the setpoint deviation from the baseline over the range of possible setpoints.

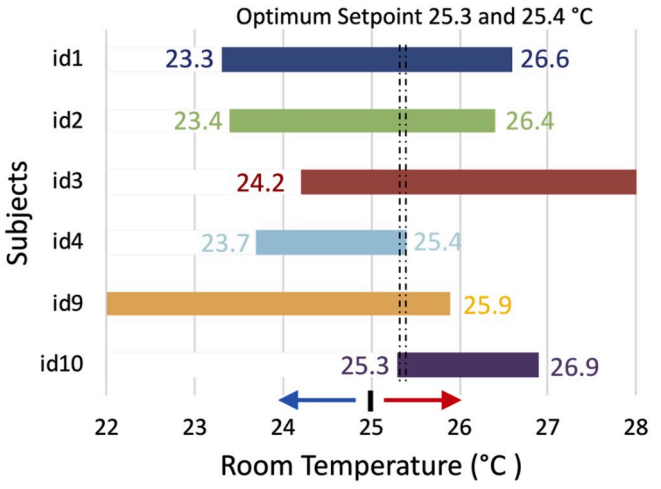

Fig. 9. Optimum Setpoint Selection Using Strategy 1 (maximize the number of comfortable occupants).

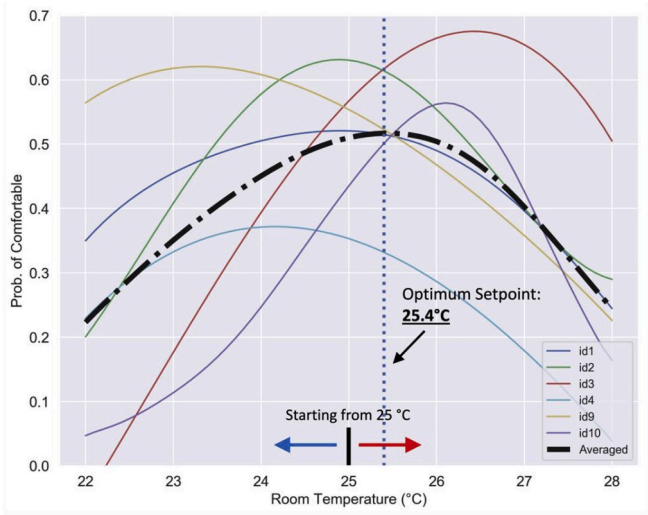

Fig. 10. Optimum Setpoint Selection Using Strategy 2 (maximize the average comfort probability when multiple setpoints yield the same number of comfortable occupants).

As R_t^* for the six subjects only includes two possible setpoints in the previous example (i.e., 25.3 and 25.4 °C), we used three subjects (subjects 1, 2, and 3) to demonstrate strategy 3 as a wider common comfort zone can be obtained. Fig. 11 shows the comfort zone (i.e., $R_t^* \in [24.2, 26.4]$, denoted in yellow) and comfort probability of these three example subjects.

Using strategy 1, any setpoint within the comfort zone R_t^* can be selected as these three subjects are all comfortable in this range. More specifically, the lower bound 24.2 °C is optimum in heating seasons due to its lower HVAC energy consumption, and vice versa for cooling seasons. When using strategy 2, setpoint 25.5 °C is selected as it achieves the highest average comfort probability.

For strategy 3, assuming in heating seasons, the comfort score and energy score at different setpoints in $\boldsymbol{R_t^*}$ are calculated, which are shown in Table 4. Only setpoints between 24.2 °C and 25.5 °C are presented as setpoints higher than 25.5 °C will reduce the average comfort probability while increasing the energy use. The weighted sum (denoted as $\boldsymbol{S}$) of comfort score and energy score for three example α values (i.e., $\alpha =$

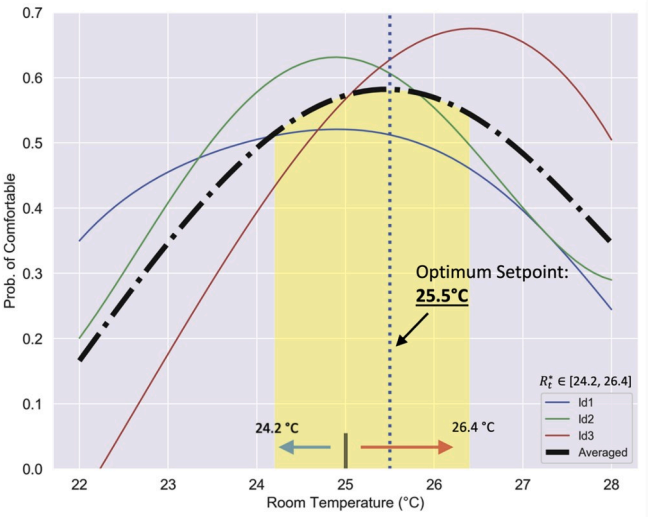

Fig. 11. The thermal comfort zone and probability for subjects 1, 2, and 3.

[1] The x-axis is reversed to represent the decreasing room temperature.

Table 4
The comfort score and energy score at different setpoints for a multi-occupancy environment with subjects 1, 2, and 3.

R_t^*	24.2	24.3	24.4	24.5	24.6	24.7	24.8
$\sum_i Prob_i(R_t^*)/n$	0.51	0.52	0.53	0.54	0.55	0.56	0.56
Comfort_score (1)	0.88	0.90	0.92	0.93	0.94	0.96	0.97
$R_{base} - R_t^*$	−2.2	−2.3	−2.4	−2.5	−2.6	−2.7	−2.8
Energy_score (2)	0.37	0.38	0.40	0.42	0.43	0.45	0.47
R_t^*	24.9	25.0	25.1	25.2	25.3	25.4	25.5
$\sum_i Prob_i(R_t^*)/n$	0.57	0.57	0.57	0.58	0.58	0.58	0.58
Comfort_score (1)	0.98	0.98	0.98	0.99	0.99	1.00	1.00
$R_{base} - R_t^*$	−2.9	−3	−3.1	−3.2	−3.3	−3.4	−3.5
Energy_score (2)	0.48	0.50	0.52	0.53	0.55	0.57	0.58

Note: The scores are rounded to two decimal places.

0.3, 0.5, and 0.7) are presented in Table 5. The results suggest that 24.2 °C, 24.2 °C and 24.7 °C are the optimum setpoints when the weight α equals 0.3, 0.5 and 0.7, respectively.

6. Discussion

In Section 4, personal comfort models and physiological predictive models are developed using multinomial logistic regression and linear mixed model, respectively. However, as explained earlier, the main contribution of this paper is the HEAT framework that consists of personal thermal comfort sensing and optimization to address the limitations in physiological sensing-based HVAC control methods. These two models, which form a subject's thermal profile, can be substituted by other modeling approaches. For example, personal comfort models can also be developed using multinomial mixed-effects logistic regression or Random Forest.

Section 5 demonstrates the optimum setpoint selection using three different strategies considering occupants' thermal comfort and HVAC energy consumption. Specifically, optimum setpoints in strategies 2 and 3 come from the candidate range R_t^* determined by strategy 1. In other words, optimum setpoints in all strategies will always be selected on the premise that most of the subjects will feel comfortable. However, if the domain of strategy 2 is the full operational range of 22 °C–28 °C instead of the narrowed range R_t^*, setpoints associated with the highest average comfort probability may not yield the largest possible number of comfortable occupants. This scenario is illustrated in Fig. 12 where two subjects share the same environment. The overlap of two subjects' comfort zones, i.e., the common comfort zone (denoted in yellow), represents R_t^*. The result shows that setpoints corresponding to the highest average comfort probability, in these two scenarios, are outside of R_t^*. In this case, subject 4 no longer feels comfortable even though the average comfort probability is maximized.

The optimum setpoints can be updated based on the presence of subjects. For example, as shown in Fig. 13, the optimum setpoint for subjects 1 and 2 is 24.9 °C. If subject 3 joins, the setpoint should increase to 25.5 °C to accommodate the newcomer's preference for warm environments without reducing the overall comfort. This approach has implications in shared environments, such as conference rooms and offices where an optimum setpoint can be found given different combinations of thermal profiles (i.e., personal comfort models and physiological predictive models). For occupants who are outside of the common comfort zones, adaptive behaviors (e.g., putting on a jacket) or personal devices (e.g., portable heater) can be adopted to restore personal comfort without affecting others. Thermal profiles developed in this paper can also be carried by occupants as they move around places. For example, thermal profiles saved in smartphones can be retrieved when occupants scan a QR code upon entering a room or connecting to a nearby Wifi router [14]. Motion sensors or thermal cameras can also determine the presence of occupants if they have dedicated working areas [26]. For new occupants who do not have pre-trained thermal profiles, template profiles or profiles of similar occupants (e.g., occupants with similar age and weight) can be used as a starting point and updated using personal data [8,40]. Specifically, Daum et al. [8] showed that template comfort models can converge to over 70% of actual personal models with twenty thermal votes.

As subjects' skin temperature has different sensitivities in heating and cooling scenarios, thermal comfort zones and comfort probabilities can be slightly different when the room is preset at a low temperature versus a high temperature, assuming subjects achieved the steady-state conditions in both cases. This scenario is demonstrated in Fig. 14 and Fig. 15, which show the differences in thermal comfort zones and probabilities when room temperature starts from the high or low baseline setpoints, especially for subjects 1 and 4 whose comfort zones and probabilities can shift by over 1 °C. These differences are mainly caused by the psychological perception in which the reference temperature that people compare with has changed in the transient environment. Subjects' evaluation of thermal sensation is relative to their initial thermal states at the high or low setpoints instead of the absolute room temperature.

It is worth noting that this paper is not meant to suggest a specific setpoint for buildings like industry standards as the optimum setpoints can be different for other human subjects, built environments and HVAC systems, seasons, locations, etc. However, the proposed HEAT framework can be adopted by researchers and HVAC engineers to develop their own thermal profiles and determine the optimum setpoint in different research settings.

Three limitations of this study should be acknowledged. First, when modeling personal comfort, the environmental parameter includes only air temperature as it is directly controlled by HVAC systems. However, other factors, such as radiant temperature and air velocity, can also be measured and applied in the comfort sensing and control loop. Second, in the experiment, the skin temperature data are collected from sedentary subjects who have a low workload level. As a result, the physiological predictive model may not be valid when extrapolated to subjects in high workload or metabolic rate situations. In future studies, if subjects' skin temperature data at different workload conditions are collected following similar methods explained in this study, the proposed approach can not only select the optimum setpoint for a given group of people, but also dynamically determine the setpoint over time according to subjects' workload. Third, strategy 3 needs further investigations in shoulder seasons as cooling and heating can have different energy consumption, which affects the energy score.

Table 5
Optimum setpoint selection using strategy 3 for a multi-occupancy environment with subjects 1, 2, and 3 (for $\alpha = 0.3$, 0.5, and 0.7).

R_t^*	24.2	24.3	24.4	24.5	24.6	24.7	24.8	24.9	25.0	25.1	25.2	25.3	25.4	25.5
S ($\alpha = 0.3$)	**.01**	.00	.00	-.01	-.02	-.03	-.04	-.04	-.06	-.07	-.08	-.09	-.10	-.11
S ($\alpha = 0.5$)	**.26**	.26	.26	.26	.25	.26	.25	.25	.24	.23	.23	.22	.22	.21
S ($\alpha = 0.7$)	.51	.52	.52	.53	.53	**.54**	.54	.54	.54	.53	.53	.53	.53	.53

Note: The bold number is the highest weighted score for each α value, the corresponding R_t^* is the optimum setpoint.

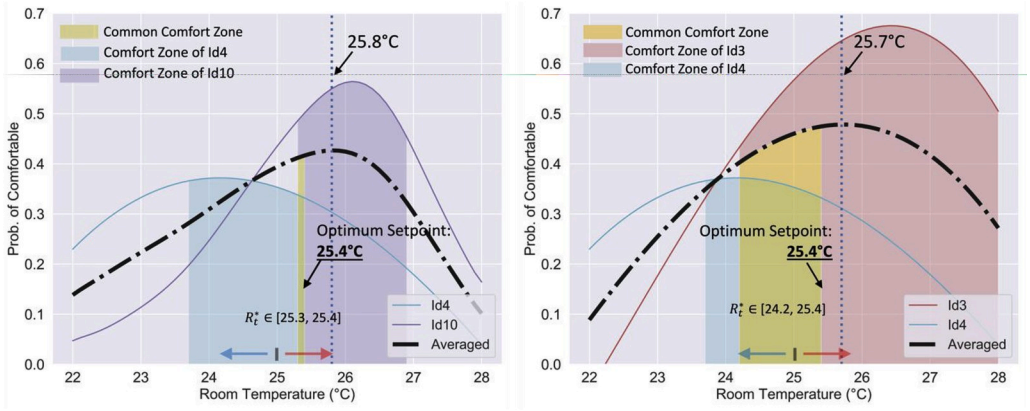

Fig. 12. The Comfort Zone and Probability for a Shared Room with Two Example Subjects (left: subjects 4 and 10; right: subjects 3 and 4).

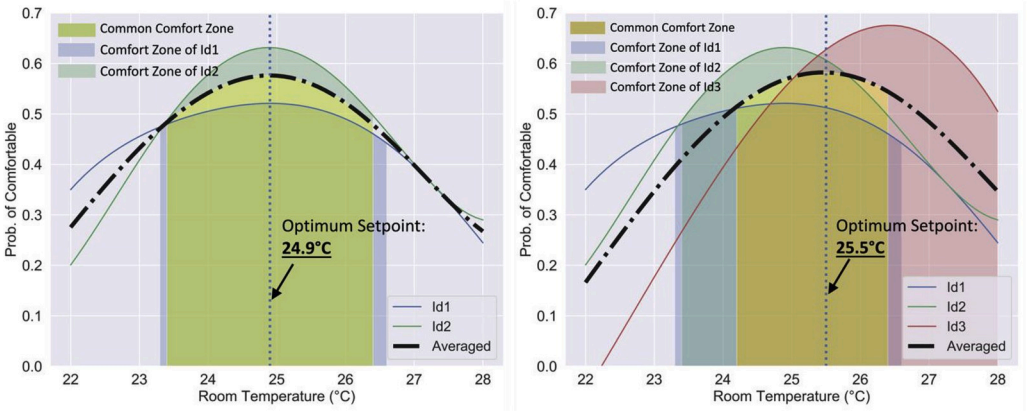

Fig. 13. The Comfort Zone and Probability for a Shared Room When a New Subject Joins (left: subjects 1 and 2; right: subject 3 joins).

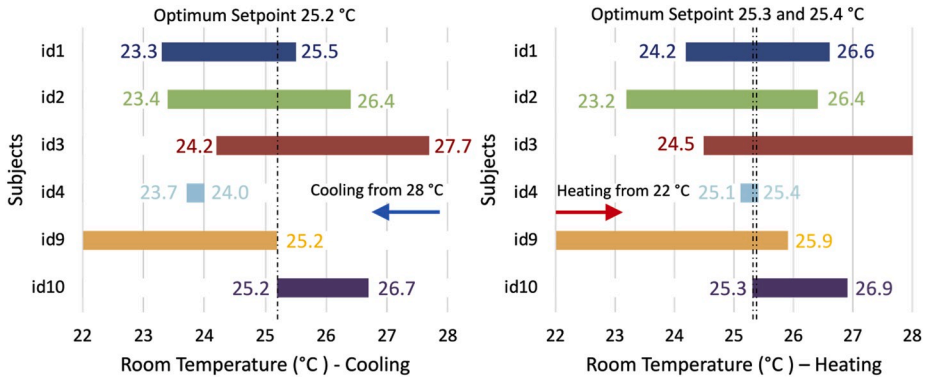

Fig. 14. Optimum Setpoint Selection Using Strategy 1 When Room Temperature Starts from the Baseline (left: start from a high setpoint; right: start from a low setpoint).

Our future study will validate the comfort and energy implications of the proposed framework on the operation of an HVAC system inside the built environment and improve control strategies using field data. Such evaluation studies will look at the impact of climate zone control, response time of HVAC systems, and effect of seasonal changes (heating versus cooling). We will capitalize on the research insights and knowledge obtained from Li et al. [14] where a smartphone app-based comfort optimization framework was developed and deployed in a real office environment. The HVAC system was controlled by a smart thermostat through cloud application programming interface (API) and group thermal satisfaction was evaluated through simulation. In Li et al. [15] and Li et al. [23]; the challenges associated with the installation of a single thermal camera and multiple camera networks (e.g., viewing distances, angles, and measurement accuracy) in the built environment were discussed, respectively.

7. Conclusions

This paper proposes the Human Embodied Autonomous Thermostat (HEAT) framework which leverages human occupants as an embodiment of smart and connected thermostats to optimize occupancy-focused HVAC operations for improved overall thermal satisfaction and reduced energy use while maintaining comfort in multi-occupancy spaces. The proposed framework consists of a sensing step which

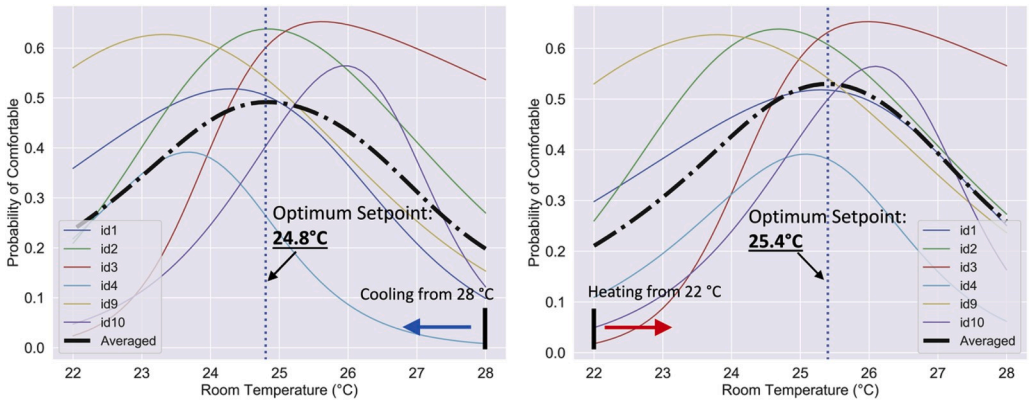

Fig. 15. Optimum Setpoint Selection Using Strategy 2 When Room Temperature Starts from the Baseline (left: start from a high setpoint; right: start from a low setpoint).

predicts occupants' thermal comfort using human physiological data, and an optimization step which determines the optimum setpoint for a multi-occupancy environment considering comfort and energy use. To this end, the proposed framework integrates personal comfort models and physiological predictive models to evaluate each occupant's thermal comfort at different setpoints. Thermal comfort in this paper can be represented in two forms, i.e., thermal comfort zone and comfort probability. Based on these two metrics, three HVAC control strategies, which leverage (1) thermal comfort zone; (2) thermal comfort zone and probability, and (3) thermal comfort zone, probability, and energy use, are compared to demonstrate the setpoint selection for a group of occupants.

This paper provides insights into proactively determining the optimum setpoint in physiological sensing-based HVAC control and has the merits of reducing discomfort time and oscillation of setpoints. After the initial setpoint optimization using the proposed framework, if physiological sensing or thermal votes from occupants indicate that further setpoint adjustments are needed, the setpoint can be updated following the human-in-the-loop schema introduced in Section 2.2 to fine-tune the thermal environment. The proposed HEAT framework that couples the physiological sensing and setpoint optimization can serve as a basis for automated environment control to improve human experience, well-being, and building energy efficiency.

Declaration of competing interest

The authors declare that they have no known competing financial interests or personal relationships that could have appeared to influence the work reported in this paper.

Acknowledgments

The authors would like to acknowledge the financial support for this research received from the U.S. National Science Foundation (NSF) CBET 1349921 and CBET 1804321. Any opinions and findings in this paper are those of the authors and do not necessarily represent those of the NSF. The authors would like to thank all subjects who participated in the experimental studies.

References

[1] L. Fang, D.P. Wyon, G. Clausen, P.O. Fanger, Impact of indoor air temperature and humidity in an office on perceived air quality, SBS symptoms and performance, Indoor Air 14 (2004) 74–81.
[2] C.A. Roulet, N. Johner, F. Foradini, P. Bluyssen, C. Cox, E. de Oliveira Fernandes, C. Aizlewood, Perceived health and comfort in relation to energy use and building characteristics, Build. Res. Inf. 34 (5) (2006) 467–474.
[3] X. Wang, D. Li, C.C. Menassa, V.R. Kamat, Investigating the effect of indoor thermal environment on occupants' mental workload and task performance using electroencephalogram, Build. Environ. 158 (2019) 120–132.
[4] X. Wang, D. Li, C.C. Menassa, V.R. Kamat, Investigating the neurophysiological effect of thermal environment on individuals' performance using electroencephalogram, in: Computing in Civil Engineering 2019: Smart Cities, Sustainability, and Resilience, American Society of Civil Engineers, Reston, VA, 2019, pp. 598–605.
[5] D. Li, C.C. Menassa, V.R. Kamat, A personalized HVAC control smartphone application framework for improved human health and well-being, in: Computing in Civil Engineering, 2017, pp. 82–90.
[6] P.O. Fanger, Thermal Comfort. Analysis and Applications in Environmental Engineering. *Thermal Comfort. Analysis and Applications in Environmental Engineering*, 1970.
[7] R. De Dear, G.S. Brager, Developing an Adaptive Model of Thermal Comfort and Preference, 1998.
[8] D. Daum, F. Haldi, N. Morel, A personalized measure of thermal comfort for building controls, Build. Environ. 46 (1) (2011) 3–11.
[9] V.L. Erickson, A.E. Cerpa, Thermovote: participatory sensing for efficient building hvac conditioning, in: Proceedings of the Fourth ACM Workshop on Embedded Sensing Systems for Energy-Efficiency in Buildings, ACM, 2012, pp. 9–16.
[10] M. Feldmeier, J.A. Paradiso, Personalized HVAC control system, in: 2010 Internet of Things (IOT), IEEE, 2010, pp. 1–8.
[11] F. Jazizadeh, A. Ghahramani, B. Becerik-Gerber, T. Kichkaylo, M. Orosz, Human-building interaction framework for personalized thermal comfort-driven systems in office buildings, J. Comput. Civ. Eng. 28 (1) (2013) 2–16.
[12] S. Purdon, B. Kusy, R. Jurdak, G. Challen, Model-free HVAC control using occupant feedback, in: 38th Annual IEEE Conference on Local Computer Networks-Workshops, IEEE, 2013, pp. 84–92.
[13] W. Jung, F. Jazizadeh, T.E. Diller, Heat flux sensing for machine-learning-based personal thermal comfort modeling, Sensors 19 (17) (2019) 3691.
[14] D. Li, C.C. Menassa, V.R. Kamat, Personalized human comfort in indoor building environments under diverse conditioning modes, Build. Environ. 126 (2017) 304–317.
[15] D. Li, C.C. Menassa, V.R. Kamat, Non-intrusive interpretation of human thermal comfort through analysis of facial infrared thermography, Energy Build. 176 (2018) 246–261.
[16] A. Aryal, B. Becerik-Gerber, A Comparative Study of Predicting Individual Thermal Sensation and Satisfaction Using Wrist-Worn Temperature Sensor, Thermal Camera and Ambient Temperature Sensor. Building and Environment, 2019, 106223.
[17] T. Chaudhuri, D. Zhai, Y.C. Soh, H. Li, L. Xie, Thermal comfort prediction using normalized skin temperature in a uniform built environment, Energy Build. 159 (2018) 426–440.
[18] Z. Deng, Q. Chen, Development and validation of a smart HVAC control system for multi-occupant offices by using occupants' physiological signals from wristband, Energy Build. 214 (2020), 109872, https://www.sciencedirect.com/science/article/pii/S0378778819336060?casa_token=m4kcevlkVO0AAAAA:LC1KmfosUPdeTv8bgcse1O2GosfLoLp2Bea5Xqau6m_2I8UhpVJr46IshGvKqDSRg3mqvxpMBY0.
[19] A. Ghahramani, G. Castro, B. Becerik-Gerber, X. Yu, Infrared thermography of human face for monitoring thermoregulation performance and estimating personal thermal comfort, Build. Environ. 109 (2016) 1–11.
[20] F. Jazizadeh, W. Jung, Personalized thermal comfort inference using RGB video images for distributed HVAC control, Appl. Energy 220 (2018) 829–841.
[21] W. Jung, F. Jazizadeh, Non-intrusive detection of respiration for smart control of HVAC system, in: Computing in Civil Engineering 2017, 2017, pp. 310–317.
[22] W. Jung, F. Jazizadeh, Human-in-the-loop HVAC operations: a quantitative review on occupancy, comfort, and energy-efficiency dimensions, Appl. Energy 239 (2019) 1471–1508.
[23] D. Li, C.C. Menassa, V.R. Kamat, Robust non-intrusive interpretation of occupant thermal comfort in built environments with low-cost networked thermal cameras, Appl. Energy 251 (2019), 113336.
[24] S. Liu, S. Schiavon, H.P. Das, M. Jin, C.J. Spanos, Personal thermal comfort models with wearable sensors, Build. Environ. 162 (2019), 106281.

[25] D. Wang, H. Zhang, E. Arens, C. Huizenga, Observations of upper-extremity skin temperature and corresponding overall-body thermal sensations and comfort, Build. Environ. 42 (12) (2007) 3933–3943.
[26] D. Li, C.C. Menassa, V.R. Kamat, Thermal and RGB-D sensor fusion for non-intrusive human thermal comfort assessment, in: CIB World Building Congress 2019, 2019. Hong Kong (No. 2019).
[27] X. Wang, D. Li, C.C. Menassa, V.R. Kamat, Can infrared facial thermography disclose mental workload in indoor thermal environments?, in: Proceedings of the 1st ACM International Workshop on Urban Building Energy Sensing, Controls, Big Data Analysis, and Visualization, 2019, pp. 87–96.
[28] W. Jung, F. Jazizadeh, Comparative assessment of HVAC control strategies using personal thermal comfort and sensitivity models, Build. Environ. 158 (2019) 104–119.
[29] A. Ghahramani, C. Tang, B. Becerik-Gerber, An online learning approach for quantifying personalized thermal comfort via adaptive stochastic modeling, Build. Environ. 92 (2015) 86–96.
[30] S. Lee, J. Joe, P. Karava, I. Bilionis, A. Tzempelikos, Implementation of a self-tuned HVAC controller to satisfy occupant thermal preferences and optimize energy use, Energy Build. 194 (2019) 301–316.
[31] J. Kim, Y. Zhou, S. Schiavon, P. Raftery, G. Brager, Personal comfort models: predicting individuals' thermal preference using occupant heating and cooling behavior and machine learning, Build. Environ. 129 (2018) 96–106.
[32] D. Li, C.C. Menassa, V.R. Kamat, Feasibility of low-cost infrared thermal imaging to assess occupants' thermal comfort, in: International Conference on. Computing in Civil Engineering (i3CE): Smart Cities, Sustainability, and Resilience, 2019.
[33] M. Luo, J. Xie, Y. Yan, Z. Ke, P. Yu, Z. Wang, J. Zhang, Comparing Machine Learning Algorithms in Predicting Thermal Sensation with ASHRAE Comfort Database II, Energy and Buildings, 2020, 109776.
[34] Z. Wang, J. Wang, Y. He, Y. Liu, B. Lin, T. Hong, Dimension analysis of subjective thermal comfort metrics based on ASHRAE Global Thermal Comfort Database using machine learning, J. Build. Eng. 29 (2020), 101120.
[35] L. Breiman, Random forests, Mach. Learn. 45 (1) (2001) 5–32.
[36] S. Lee, P. Karava, A. Tzempelikos, I. Bilionis, Inference of thermal preference profiles for personalized thermal environments with actual building occupants, Build. Environ. 148 (2019) 714–729.
[37] G. James, D. Witten, T. Hastie, R. Tibshirani, An Introduction to Statistical Learning, vol. 112, springer, New York, 2013.
[38] FLIR, Lepton engineering Datasheet, Retrieved from, https://www.flir.com/globalassets/imported-assets/document/flir-lepton-engineering-datasheet.pdf, 2018.
[39] B. Winter, Linear Models and Linear Mixed Effects Models in R with Linguistic Applications, 2013 arXiv preprint arXiv:1308.5499.
[40] J. Wu, C. Shan, J. Hu, J. Sun, A. Zhang, Rapid establishment method of a personalized thermal comfort prediction model, July, in: 2019 41st Annual International Conference of the IEEE Engineering in Medicine and Biology Society (EMBC), IEEE, 2019, pp. 3383–3386.
[41] W. Jung, F. Jazizadeh, Vision-based thermal comfort quantification for HVAC control, Build. Environ. 142 (2018) 513–523.
[42] A. Aryal, B. Becerik-Gerber, Skin Temperature Extraction Using Facial Landmark Detection and Thermal Imaging for Comfort Assessment, Proceedings of the 6th ACM International Conference on Systems for Energy-Efficient Buildings, Cities, and Transportation (2019) 71–80.